PROCEEDINGS OF SCIENCE

An overview of recent ATLAS results

Irena Nikolic-Audit, on behalf of the ATLAS Collaboration*

Laboratoire de Physique Nucléaire et de Hautes Energies (LPNHE), UPMC, Université Paris-Diderot, CNRS/IN2P3, Paris, France
E-mail: nikolic@lpnhe.in2p3.fr

The ATLAS experiment at the LHC collider has been successfully taking data since the end of 2009, both in proton-proton collisions at center of mass energies of 7 and 8 TeV, and in heavy ion collisions. The ATLAS detector has been designed to cover a wide range of physics topics, from the search for the Higgs boson, precision measurements of Standard Model physics, to heavy flavor physics, and to maximize the potential for the discovery of new physics. In this presentation, some of the most important recent ATLAS results will be given for the Standard Model measurements, for the searches for supersymmetry and exotica, and for the heavy ion results. All of the results concerning the properties of the newly discovered Higgs boson are presented in a separate contribution in these proceedings.

The XXI International Workshop High Energy Physics and Quantum Field Theory,
June 23 - June 30, 2013
Saint Petersburg Area, Russia

*Speaker.

PoS(QFTHEP 2013)001

1. Introduction

The ATLAS experiment, described in [1], in one of the four large experiments at the Large Hadron Collider (LHC) [2] collider at CERN. The ATLAS detector is a multi-purpose particle physics detector with forward-backward symmetric cylindrical geometry. The detector has been operated with very high efficiency (93%), and 95.8% of data recorded in 2012 were declared as being good for physics analysis using all subdetectors and triggers. During the year 2012, ATLAS recorded data corresponding to an integrated luminosity of 20.7 fb^{-1} at the center of mass energy of 8 TeV, which is the highest energy ever achieved at a particle collider. In 2011, 4.8 fb^{-1} were recorded at the center of mass energy of 7 TeV. Collisions with lead-lead and proton on lead were also recorded during the years 2010, 2011, 2012 and 2013. Using all this data, ATLAS has performed a very wide range of physics analyses, some of which are reviewed in these proceedings. One of the main challenges during the 2012 data taking was the high pile-up rate: the number of peak interactions per crossing was higher than the experiment's design value of 23, which was expected to be reached at a luminosity of $\mathscr{L} = 10^{34}s^{-1}cm^{-2}$. The peak luminosity in 2012 was $\mathscr{L} = 7.7 \times 10^{33}s^{-1}cm^{-2}$. In order to cope with this large pile up, it is necessary to have robust fast triggers, to optimize the reconstruction and identification of objects, to have a precise modeling of the pile up in the Monte Carlo, and to have improvements in computing models in order to be able to handle large trigger rates and large event sizes. All of this was achieved by ATLAS.

The ATLAS physics results can be divided into four categories: Higgs physics; QCD studies, precision measurements and tests of the Standard Model including top quark physics; searches for the physics beyond the Standard Model; heavy ion physics. All of the results regarding the Higgs boson are covered in a separate contribution in these proceedings [3]. More details about other ATLAS results can also be found in the talks of my colleagues at this conference and at the ATLAS public results page [4]. In each of the sub-fields, only a few recent results are detailed, and a summary is given.

2. Standard Model Physics

There have been major advances in the predictions for Standard Model processes. The largest improvements are coming from theory, with new NLO and NNLO calculations. Progress has also been made on improving Geant 4 simulations and fine tuning of event generators. Figure 1 shows the summary of several Standard Model (SM) production cross sections measured by ATLAS at 7 and 8 TeV and compared to the theoretical predictions. The cross sections are well understood over five orders of magnitude and the experimental precision of data starts to challenge the theoretical uncertainty. All of the above make the precision tests of SM production processes at the LHC possible.

2.1 QCD measurements

As QCD processes are the most abundant ones at the LHC, a very good understanding of them is necessary: beyond their intrinsic interest, they constitute the largest background for the Higgs boson or for the searches for new physics phenomena. From the events with jets, perturbative (pQCD) and non-perturbative QCD can be tested, the parameters of the theory (α_S, parton density

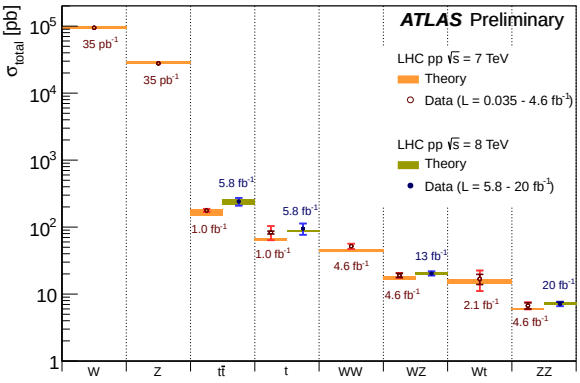

Figure 1: Summary of several Standard Model total production cross section measurements compared to the corresponding theoretical predictions [5]. The dark colored error bar represent the statistical uncertainty, the lighter colored one represents the full uncertainty, including the systematics and the luminosity one.

functions or PDFs, ..) can be extracted, and Monte Carlo models can be tuned. ATLAS has performed a wide range of studies of QCD phenomena: jet multiplicity ratios from which the value of α_S has been extracted [7], inclusive isolated photon cross sections [8] have been measured, isolated photon and photon-jet dynamics studies [9] have been done. The value of α_S extracted from the ratio of three-jet events to two jet events cross sections, is consistent with the current world average and with other experiments.

The differential inclusive jet production cross section has been measured in ATLAS, at two different energies: at 2.76 TeV using an integrated luminosity of 0.2 pb^{-1}, and at 7 TeV [10]. This is done covering a wide range of jet rapidity, up to $|y| < 4.4$. Jets are defined using the anti-k_t algorithm, with two different radius parameters of R=0.4 and R=0.6. The inclusive jet double-differential cross-section is presented as a function of the jet transverse momentum p_T and jet rapidity in Figure 2(a). The ratio of the inclusive jet cross-section at $\sqrt{s} = 2.76$ TeV to the inclusive jet cross-section measurement at $\sqrt{s} = 7$ TeV is calculated as a function of both the transverse momentum and the dimensionless quantity $x_T = 2p_T/\sqrt{s}$, in bins of jet rapidity. The systematic uncertainties on the ratios are significantly reduced due to the cancellation of correlated uncertainties in the two measurements giving a more stringent test of pQCD and extra sensitivity to PDFs is obtained. Measurements are compared to the prediction from NLO pQCD calculations corrected for non-perturbative effects, and NLO Monte Carlo simulation. The comparison is performed using different proton PDF sets (see Figure 2(b)). An NLO pQCD fit has been performed on the data sets corresponding to 2.76 TeV and 7 TeV, together with the HERA I data, in order to constrain the proton PDFs. Figure 3(a) shows the results for the gluon distribution for different cases. HERA data alone are shown in yellow and the results including different sets of ATLAS data are shown in lines. It can be seen from that figure that the fitted gluon distribution becomes harder and the sea quark becomes softer when the ATLAS jet data is used. From the Figure 3(b), we can see that the data are well described by the prediction based on the refit PDFs after the addition of jet data, with a particular improvement in the forward region at high rapidity |y|, corresponding to high parton x.

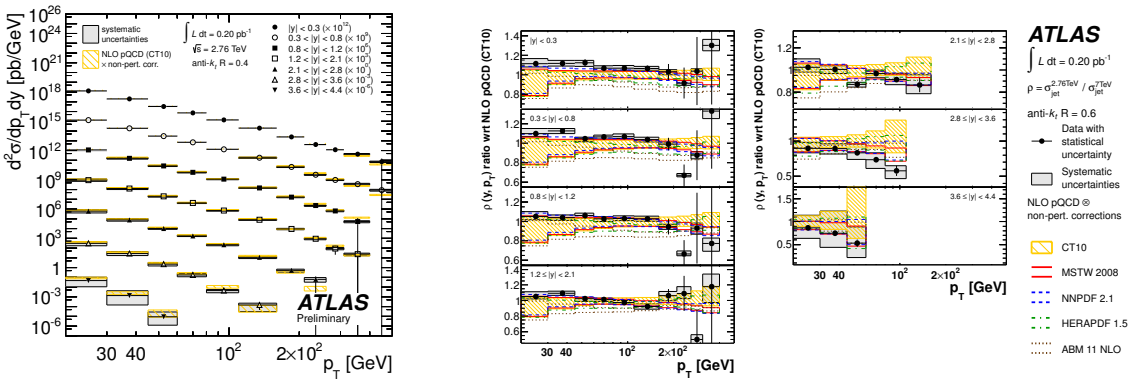

(a) (b)

Figure 2: (a) Inclusive jet cross section as a function of p_T for center of mass energy of 2.76 TeV for R=0.6 [10]. (b) Ratio of the inclusive jet cross section at 2.76 TeV to the one at 7 TeV, shown as a double ratio to the theoretical prediction calculated with CT10 PDFs as a function of the jet p_t in bins of jet rapidity [10].

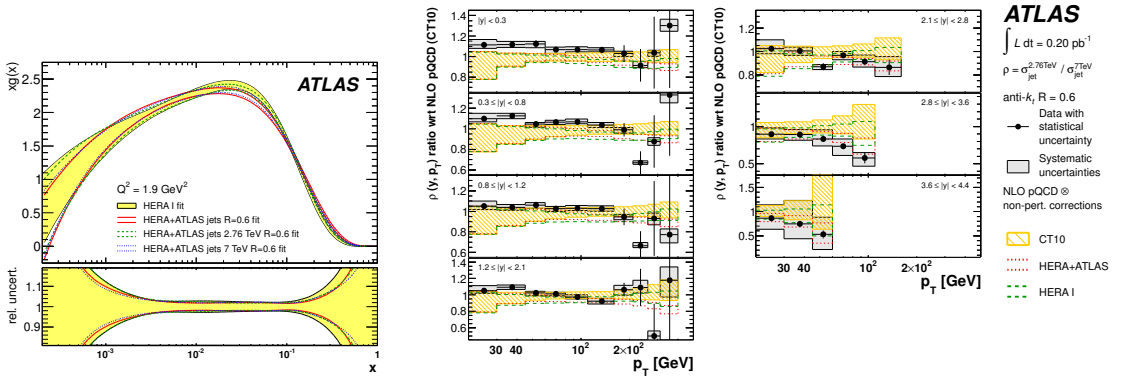

(a) (b)

Figure 3: (a) The extracted gluon distribution as a function of x for various sets of ATLAS and HERA data at $Q^2 = 1.9$ GeV^2 [10]. (b) Comparison of NLO pQCD jet cross section ratio at 2.76 TeV to 7 TeV, calculated with the CT10 PDF set, the fitted PDF set using HERA data only and the one using HERA data and the ATLAS jet data. Predictions are normalized to the one using the CT10 PDF set [10].

2.2 Forward-Backward Asymmetry of the Z/$\gamma*$

The electroweak theory predicts an asymmetry in the direction of the leptons produced in the $q\bar{q} \to Z/\gamma^* \to l^+l^-$ process with respect to the direction of the incoming quarks, in the rest frame of the dilepton l^+l^- system. This forward-backward asymmetry, $A_{FB} = \frac{\sigma_F - \sigma_B}{\sigma_F + \sigma_B}$, was measured and was used to determine the effective weak mixing angle using the decays of the Z boson into electrons and muons. The unknown incoming quark direction is approximated by the longitudinal boost of the lepton pair in the laboratory frame. The combination of the two decay channel yields a value of $\sin^2\theta_W^{\text{eff}} = 0.2297 \pm 0.0004(\text{stat}) \pm 0.0009(\text{syst})$ [11], which is as precise as the measurement at D0 (the previous most precise result at hadron colliders), and is in agreement with the world average.

2.3 Diboson Physics

The measurements of electroweak boson production provide very important tests of the SM. Furthermore, diboson events are significant and irreducible backgrounds for the Higgs boson and exotica searches. Deviations in cross sections or the existence of neutral triple gauge couplings (TGC), forbidden in the SM, could indicate physics beyond the SM. ATLAS has performed a full scan of possible diboson processes $(W\gamma, Z\gamma, WW, WZ, ZZ)$ [12], [13], [14], [15]. Diboson cross sections have been measured at 7 and 8 TeV, and the results are shown in Figure 4 (a) for ZZ processes [12]. The results are in good agreement with the NLO calculations using MCFM [16]. Charged, neutral and anomalous triple gauge couplings have also been measured. Limits obtained for WWZ and WWγ couplings are comparable or tighter than the ones obtained at the Tevatron. In the case of the anomalous TGC shown in Figure 4 (b), limits derived in ZZZ and ZZγ channels are better than the LEP and Tevatron results.

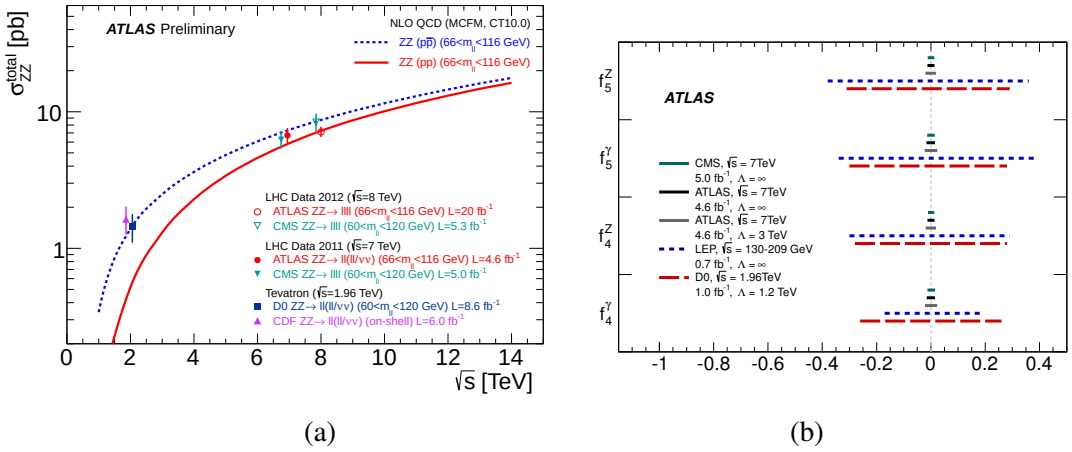

(a) (b)

Figure 4: Diboson production: (a) ZZ cross section as a function of $\sqrt{(s)}$ [12]; (b) Anomalous neutral TGC at 95% confidence intervals [14].

2.4 Top Quark Physics

The top quark is the heaviest fundamental particle observed so far and as such can play a special role in electroweak symmetry breaking. The top has large couplings to the Higgs boson, and is also the most important background to many new physics signatures and Higgs boson studies. Thus, top production has to be very well understood. At the LHC, unprecedented samples of top quarks have been produced with 5.6 million top pairs (produced mainly by gluon fusion) and 2.7 million single top events corresponding to 5fb^{-1} at 7 TeV and 21fb^{-1} at 8 TeV. The top quark almost always decays into a W boson and a b quark. Top final states are classified according to the W decay modes (which can be a hadronic or leptonic mode, the leptonic mode including the decays into electrons or muons, while the decays into tau leptons are treated separately). The top pair final state can thus be an all-hadronic, lepton+jet or dilepton final state.

2.4.1 Mass and cross section measurements

The cross section for $t\bar{t}$ pairs has been measured in all final states, and using large top samples,

differential cross sections have been measured as a function of observables sensitive to QCD predictions: $m_{t\bar{t}}$, $p_{T,t\bar{t}}$ and $y_{t\bar{t}}$. The results for cross sections measurements in various final states are shown in figure 5, at 7 and 8 TeV, and are compared to NLO and approximate NNLO calculations based on Hathor 1.2. At 8 TeV, in the lepton+jet final state the cross section is measured to be $\sigma_{t\bar{t}} = 241 \pm 2(\text{stat}) \pm 31(\text{syst}) \pm 9(\text{lumi})$ pb [17], in good agreement with the theoretical prediction which is $\sigma_{\text{theor}} = 238^{+22}_{-24}$ pb.

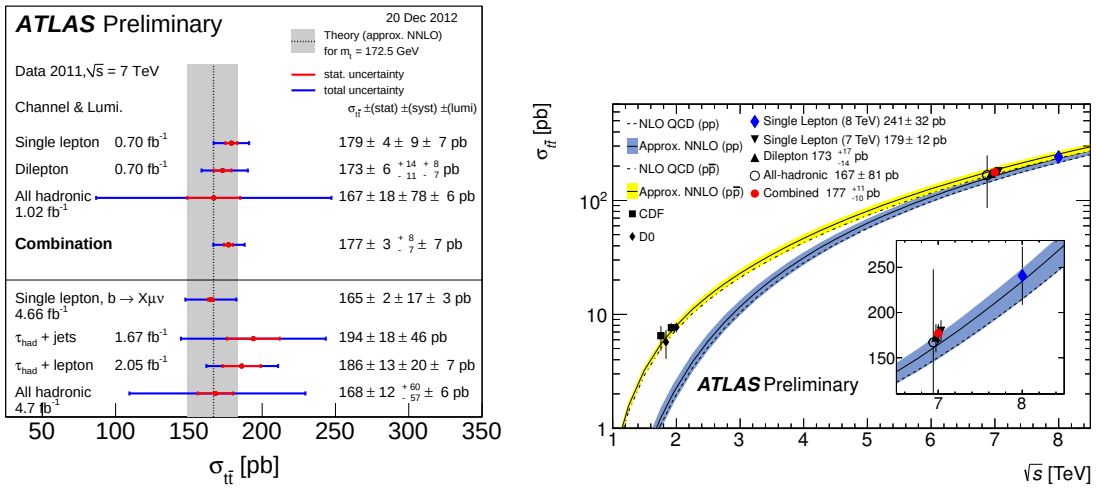

Figure 5: Top-antitop pair production cross sections in different $t\bar{t}$ final states [5].

Top quarks can also be produced at the LHC via electroweak, charged-current interactions. Single top cross sections measurements, which are of particular importance as sensitive to the Wtb vertex and to many new physics processes, have been performed in the t and W+top channels, at 7 and 8 TeV, and an upper limit has been given for the s channel [18]. The results, compared to the NNLO predictions, are shown in Figure 6 (a).

Among other measurements summarized in figure 6 (b), the top quark mass has been measured with 4.7 fb^{-1} of data at 7 TeV using the template method in the channel $t\bar{t} \to$ lepton+jets (lepton=e, μ) [19]. This analysis uses a 3-dimensional template technique which determines the top quark mass together with a global jet energy scale factor (JSF), and a relative b-jet to light-jet energy scale factor (bJSF), where light jets refers to u,d,c,s quark jets. The systematics are reduced in this analysis by 40 % with respect to the previous analysis. The top quark mass is measured to be: $m_{\text{top}} = 172.31 \pm 0.75(\text{stat}) \pm 1.35(\text{syst})$ GeV, where the statistical error includes the components due to the simultaneous fit of the JSF and bJSF.

2.4.2 W polarization in top decays

In the Standard Model, top quarks decay into a W boson and a b quark. The V-A structure of the Wtb vertex can be tested by measuring the polarization of W bosons produced in top decays. The fractions of events containing W bosons with longitudinal, left handed and right handed polarization, also called helicity fractions, are predicted at NNLO by perturbative QCD calculations. In particular, the distribution of the angle θ^* between the charged lepton and the reversed direction

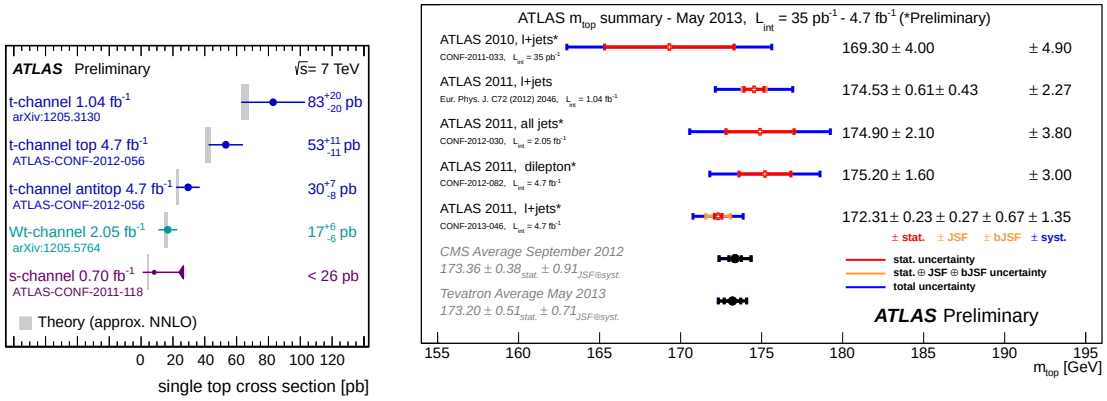

Figure 6: (a) Summary of single top cross section results in ATLAS compared to the NNLO predictions. (b) Top mass results in ATLAS [5].

of the top quark, both in the W rest frame, is sensitive to the helicity fractions. The measurement has been performed in top quark pair events, using events in which one or both W bosons decay leptonically. The data used is 35 pb^{-1} of data taken in 2010 and 2.2 fb^{-1} of data taken in 2011. A combination with a CMS measurement has been made [20] and the results, shown in the Figure 7 (a) , are consistent with the SM and are used to set limits on anomalous couplings g_L and g_R.

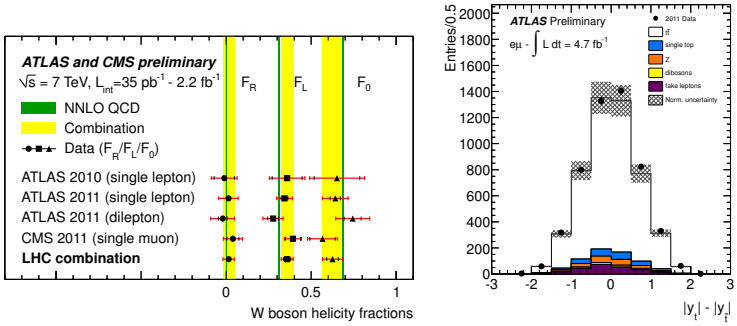

Figure 7: (a) W helicity fractions in top decays [20]. Overview of the four measurements included in the combination as well as the results of the combination. The inner and outer error bars correspond to the statistical and the total uncertainty, respectively. The green solid line indicates the predictions of NNLO QCD calculations. (b) Δy distribution for pairs of leptons in the $e\mu$ channel in charge asymmetry measurement [21] .

2.4.3 Charge asymmetry in top decays

At the LHC, the dominant production mechanism for $t\bar{t}$ production is gluon-gluon fusion which is symmetric under the exchange of top and anti-top quarks, and the asymmetric production via $q\bar{q} \to t\bar{t}g$ and $qg \to t\bar{t}q$ processes is small. Nevertheless, at NLO, QCD predicts a small excess of centrally produced antitop quarks and top quarks produced at higher absolute rapidities. $t\bar{t}$ production via $q\bar{q}$ annihilation is dominated by initial valence quarks with large momentum frac-

tions, while antiquarks coming from the sea have smaller momentum fractions. With top quarks being preferentially emitted in the direction of the initial quark in the $t\bar{t}$ rest frame, the boost into the laboratory frame drives the top quarks mainly forward or backward, while antitop quarks are kept central. New physics could enhance this effect. Asymmetries measured in $t\bar{t}$ events can be measured, and are a test of QCD and a benchmark for new physics.

The top pair charge asymmetry, defined as $A_C = \frac{N(\Delta|y|>0)-N(\Delta|y|<0)}{N(\Delta|y|>0)+N(\Delta|y|<0)}$ where $\Delta|y| = |y_t| - |y_{\bar{t}}|$ is the difference between the absolute values of the rapidities of the top and anti top quarks and N the number of events where that quantity is positive or negative, has been measured in [21] using $t\bar{t}$ events decaying to exactly two electrons or muons, two neutrinos and at least two jets using data corresponding to an integrated luminosity of 4.7 fb^{-1}. The measured value of the top quark asymmetry extracted from the combination of both the dilepton and single lepton final states is $A_C = 0.029 \pm 0.018(\text{stat}) \pm 0.014(\text{syst})$. This value is in good agreement with the MC@NLO [22] calculation which predicts 0.006 ± 0.002 for the $t\bar{t}$ based asymmetry.

2.5 Heavy Flavor Physics

Among several heavy flavour physics subjects studied in ATLAS, the angular analysis of semi-rare decays $B^0_d \to K^{0*}\mu\mu$ has been performed [23]. Angular distributions of the four-particle final states, as well as decay amplitudes, are sensitive to physics beyond the SM, as a result of the interference of new diagrams with the SM model diagrams. The decay is described by four kinematic variables: the invariant mass (q^2) of the di-muon system, and 3 angles describing the geometrical configuration of the final state shown in Figure 8(a). The differential distributions $\mathrm{d}^2\Gamma/\mathrm{d}q^2\mathrm{d}\cos\theta_L$ and $\mathrm{d}^2\Gamma/\mathrm{d}q^2\mathrm{d}\cos\theta_K$ are binned in intervals in q^2, and the values of the K^{0*} longitudinal polarisation fraction F_L and of the lepton forward-backward asymetry A_{FB} are extracted, averaged in q^2 bins. They are shown in Figure 8(b) and (c). The theoretical expectations have been calculated for the limits of small and large q^2. The analysis used 4.9 fb^{-1} of 2011 data at 7 TeV, and the results are in reasonable agreement with SM predictions.

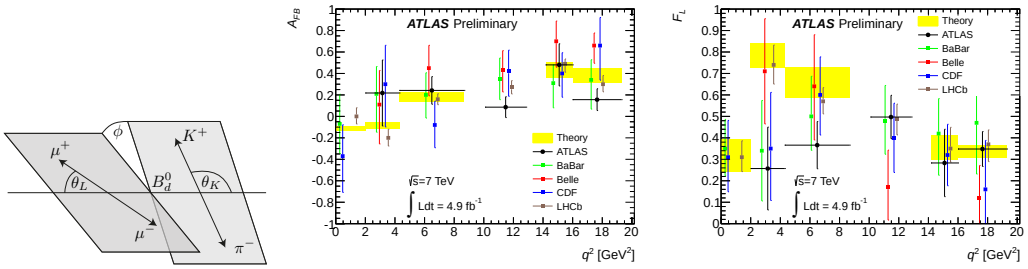

(a) (b) (c)

Figure 8: (a) Angular variable in B^0_d decays [23]. (b) Lepton forward-backward asymmetry (A_{FB}) and (c) K^{0*}longitudinal polarisation fraction F_L, including statistical and systematical uncertainties, compared to the theoretical predictions [23].

3. Beyond the Standard Model Physics

The 21 fb^{-1} of data collected at 8 TeV gives access to a new energy regime. Even though the

Standard Model has been verified better than ever before, there are still open questions to which it does not answer: the nature of dark matter, the unification of fundamental interactions etc. There is thus a need to look for physics beyond the SM. We separate the searches beyond the SM into the searches for Supersymmetry (SUSY) and the non SUSY ones.

3.1 Supersymmetry

Supersymmetry is an attractive theory beyond the SM and is its most popular extension, as SUSY particles provide a natural solution to the hierarchy problem by canceling the divergent quantum corrections to the Higgs mass. SUSY also allows unification of couplings at high energies and provides a dark matter candidate in the lightest supersymetric particle (LSP). Large parts of the MSSM parameter space have been excluded by previous searches for SUSY particles. Electroweak scale SUSY is still possible with a large mixing in the stop sector (with one light stop and one heavy one, or both below 1 TeV), or with extra matter gauge fields. The so called "natural" SUSY scenario, where there is a light chargino, neutralino and a light stop, with masses typically below the TeV, while other squarks and gluinos have typically masses above 1 TeV, is a very interesting scenario.

Throughout the years, ATLAS has set up a search strategy which maximizes the discovery potential for a variety of possible SUSY signals. These searches include searches for prompt particles in both R parity[1] conserving (RPC) and R parity violating scenarios. There are also searches for long lived particles with various ranges of lifetimes, and for monopoles. In the case of RPC scenarios, an extensive study of inclusive production of squarks and gluinos through the strong interaction, of the production of stop and sbottom squarks and of gauginos and sleptons produced through electroweak interactions has been done. Model independent searches have also been performed.

In the case of SUSY particles produced within a RPC scenario, SUSY particles are produced in pairs and there will be two LSP particles (which are the lightest neutralino $\tilde{\chi}_1^0$ in a variety of cases) escaping detection in the final state. Typical experimental signatures are thus large missing transverse momentum p_T^{miss}, and its magnitude E_T^{miss}, and final states with variable number of jets and zero or a multiple number of leptons (leptons meaning electrons or muons). Kinematic variables which distinguish betweens tails of the SM distributions and SUSY candidate events are defined, such as effective mass, boost-corrected contraverse mass.. The background has to be extremely well controlled: it is measured in control regions and propagated to signal regions through simulations. Results are often interpreted in terms of simplified models, where only one specific decay chain is considered to develop in a fraction of cases. As SUSY has many free parameters, any conversion of results into exclusion limits requires assumptions on decay chains, masses and branching ratios. No deviations from the SM predictions are observed and all of the results given are limits at 95% confidence level.

There were dedicated searches for the inclusive strong production of gluinos and first and second generation squarks, into final states with leptons or fully hadronic, in the case of MSUGRA, CMSSM or GMSB models. For example, in searches for generic RPC SUSY, in final states with no leptons, with several (2 to 6) jets and missing p_T, and in a simplified model with only gluinos and

[1] R parity is defined as $R = (-1)^{3(B-L)+2S}$ for a particle of spin S, baryon number B and lepton number L.

the lightest neutralino, gluino masses below 1350 GeV are excluded at the 95% confidence level when the lightest neutralino is massless. In a simplified model involving the strong production of squarks of the first two generations, with decays to a massless lightest neutralino, squark masses below 780 GeV are excluded. With the same final state, and with MSUGRA/CMSSM models with $\tan\beta = 30$, $A_0 = -2m_0$ and $\mu > 0$, squarks and gluinos of equal mass are excluded for masses below 1.7 TeV [24].

In the case of natural SUSY, the stop $\tilde{t}_1$ and the sbottom $\tilde{b}_1$ are the lightest colored SUSY particles. The $\tilde{t}_1$ and $\tilde{b}_1$ can be produced either via gluino mediation, or via direct production. Considering gluino-mediated stop production, the most stringent limit obtained on the gluino mass is 1.3 TeV in the case of a massless neutralino. It is achieved using searches for events with zero or at least one lepton, at least four jets and at least three b-jets [25]. In models with direct stop pair productions, the $\tilde{t}_1$ can decay in a wide variety of modes. Final states include jets, 0 , 1 or 2 leptons, and E_T^{miss}. If 100 % branching fractions are assumed for $\tilde{t}_1 \to t\tilde{\chi}_1^0$, or $\tilde{t}_1 \to t\tilde{\chi}_1^\pm$, $\tilde{t}_1$ below 600-700 GeV are excluded, as is summarized in Figure 9 for various final states.

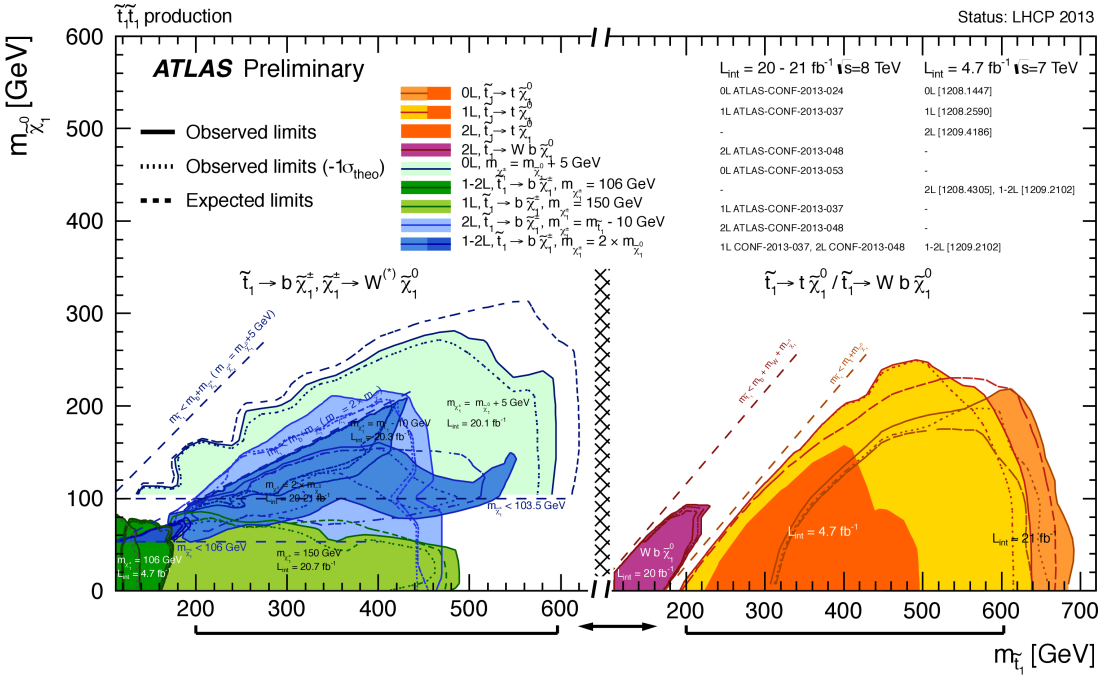

Figure 9: Summary of the dedicated searches for stop quark production based on 20-21 fb^{-1} of pp collision data taken at 8 TeV and 4.7 fb^{-1} at 7 TeV [5]. Exclusion limits are at 95% CL in the stop-neutralino plane. Several decay modes are shown.

SUSY particles produced by the electroweak interaction are the charginos and the neutralinos. The direct production gives either pairs of charginos ($\tilde{\chi}_1^-\tilde{\chi}_1^+$) or a production of a chargino and next to lightest neutralino ($\tilde{\chi}_1^\pm\tilde{\chi}_2^0$). In analysis where SUSY particles are produced via the electroweak interaction, and the final states signature is 3 leptons and E_T^{miss}, chargino and heavy neutralino masses are excluded up to 600 GeV if the decays are via sleptons and up to 315 GeV if the decays are via W^*/Z^* bosons into a massless lightest neutralino [26].

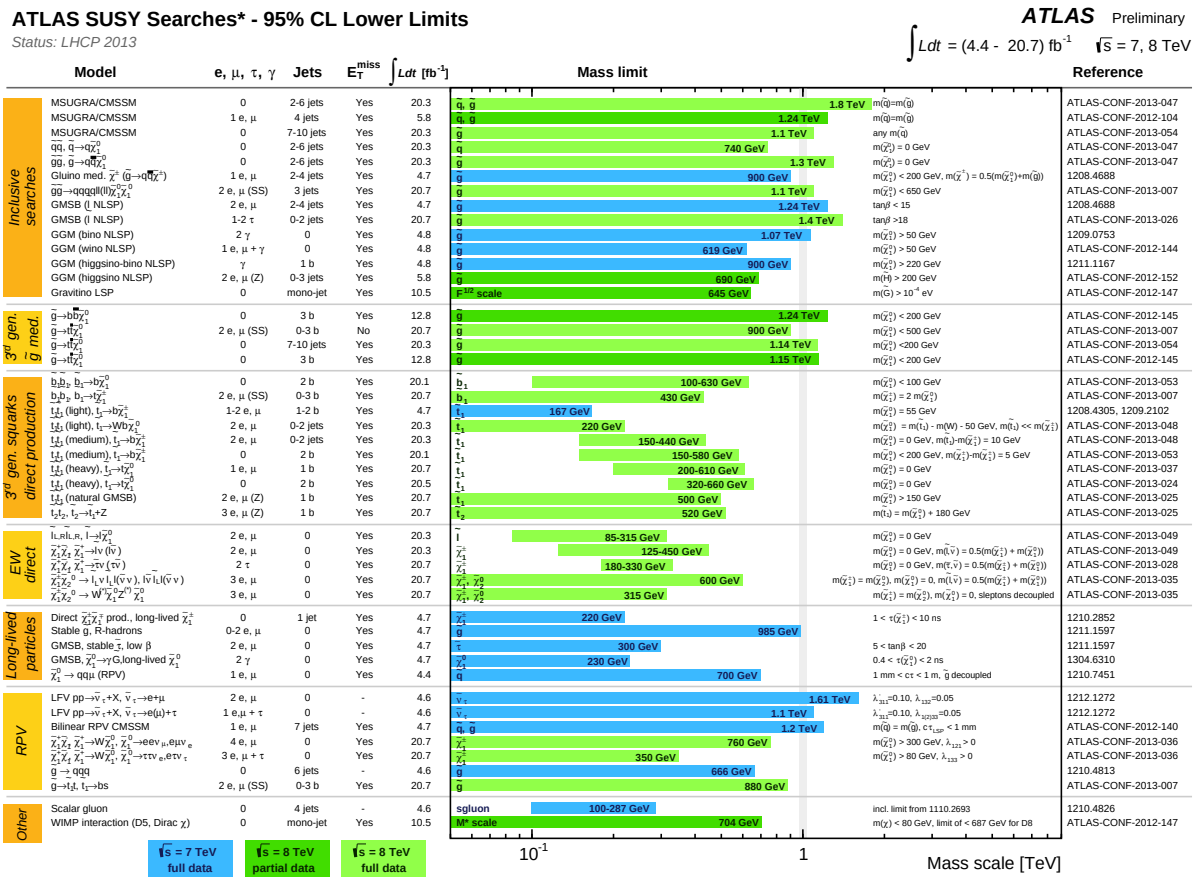

Figure 10: Summary of ATLAS exclusions limits for SUSY searches [5].

The summary of all of the ATLAS SUSY searches, as of May 2013, is given in Figure 10.

3.2 Exotica

Besides SUSY, several other extensions of the SM have been developed. Amongst the available theories are the ones implying extra dimensions, technicolor, GUT, leptoquarks, compositeness, heavy and vector like quarks etc. All of these theories predict new particles, or new states of known particles. In the presence of many possible theories, with many particles, production and decay modes, a search strategy is to look for experimental signatures such as monojets, dark matter pair production, excited leptons, vector like quarks and heavy resonances. All of these, and other signatures, with results summarized in Figure 11, have been looked for in ATLAS.

Searches for heavy resonances with dileptons, dibosons and dijets have been made. From dijet resonant state studies, excited quarks with masses $m(q^*)$< 3.84 TeV have been excluded [27]. The dilepton (lepton meaning electron or muon) state is one of the cleanest signatures, with a very low background, the main challenge being the resolution on the transverse momentum of the very energetic lepton. ATLAS has looked for this signature [28]. Figure 12 (a) shows the expected and the observed dimuon spectrum. A Sequential Standard Model (SSM) Z' boson with Standard

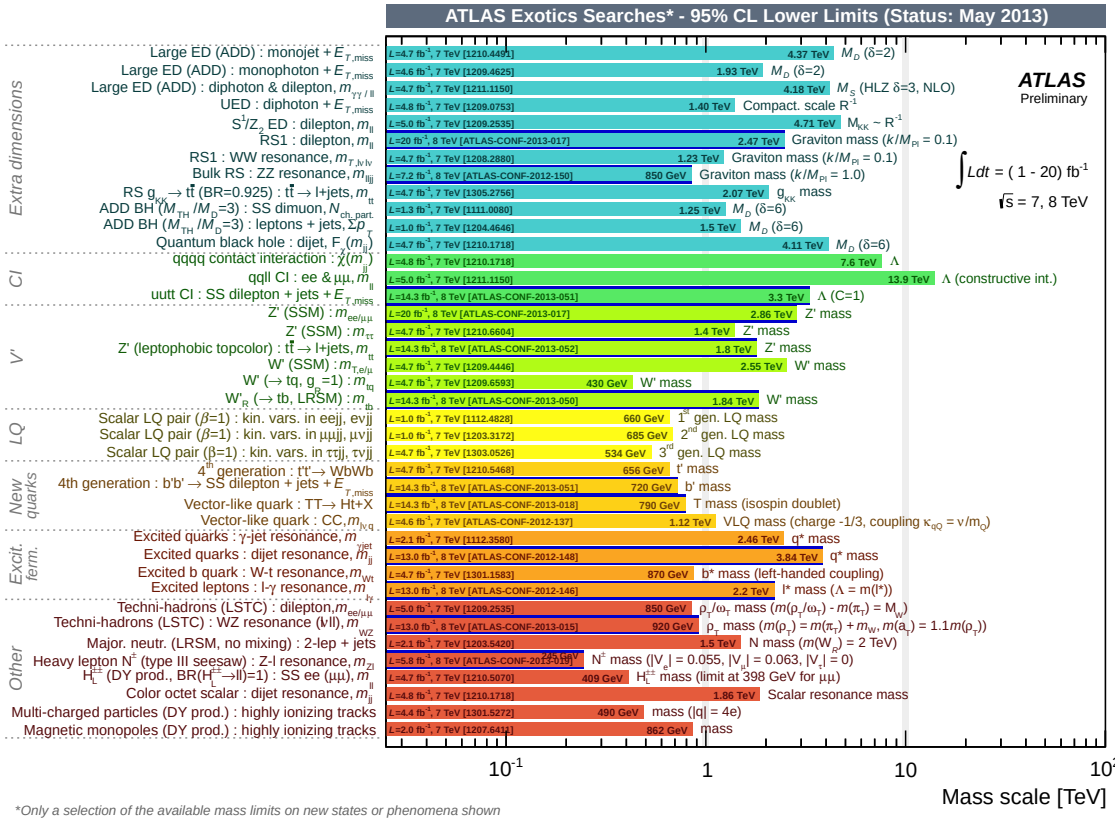

Figure 11: Summary of ATLAS exclusions limits for non-SUSY searches [5].

Model couplings to fermions is excluded at 95 % C.L. for m< 2.86 TeV when e^+e^- and $\mu^+\mu^-$ channels are combined. In the same analysis, the search for the Randall Sundrum graviton G* has been performed, and for a coupling $k/\bar{M}_{PL} = 0.1$, k being the space time curvature in extra dimensions, the limit of $m(G^*)$< 2.47 TeV is obtained. In the case of a E6 gauge group, a Z'_ϕ with m<2.38 TeV is excluded.

A search for WZ diboson resonances has been done in [29], in the fully leptonic final state. Such resonnances are predicted in Technicolor models, with technirho mesons and in composite Higgs models with heavy gauge bosons. The WZ spectrum is shown in Figure12(b). The following limits are derived: m(ρ_T) $<$ 920 GeV and $m(W') < 1.18$ TeV, with 13fb^{-1} of data.

Models with an extra family of heavy chiral fermions have also been studied. In the quark sector, the new weak-isospin doublet contains heavy up-type T and down-type B quarks which are nearly degenerate in mass and mix with the lighter quarks via an extended CKM matrix. Vector-like quarks are expected to mix preferentially with third generation quarks and as a result they present a rich phenomenology. The search for the T vector like top quark partner through the decay modes $T \to Wb$, $T \to Zb$, and $T \to Ht$ has been performed. For a chiral fourth generation quark, and under the assumption of a branching ratio BR($T \to Wb$)=1, a mass lower than 740 GeV is excluded at 95% CL. For vector-like T quarks, and under the assumption that only the $T \to Wb$,

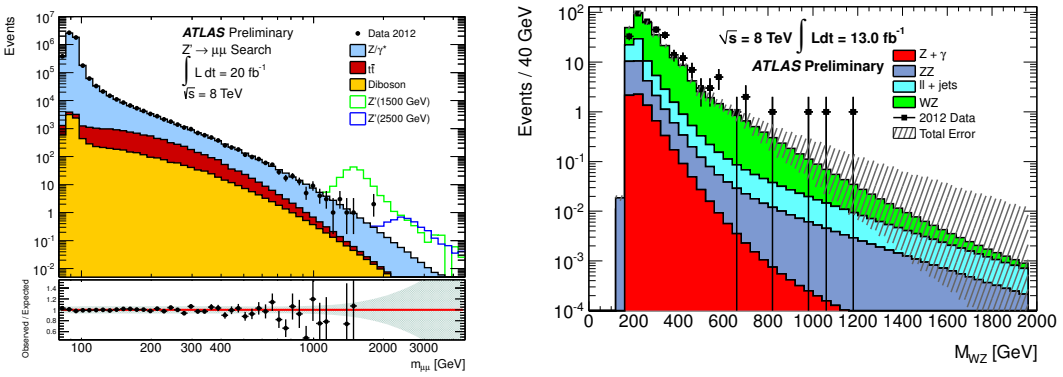

(a) (b)

Figure 12: (a) Search for heavy dilepton resonances [28]. Predicted and observed dilepton invariant mass spectrum, in the dimuon channel with two Z' signals at two different masses. (b) Search for diboson WZ resonances, in a 3 lepton final state [29].

$T \to Zt$ and $T \to Ht$ decay modes contribute, 95% CL upper limits are derived for various masses in the two-dimensional plane of BR$(T \to Wb)$ versus BR$(T \to Ht)$ and are shown in Figure 13.

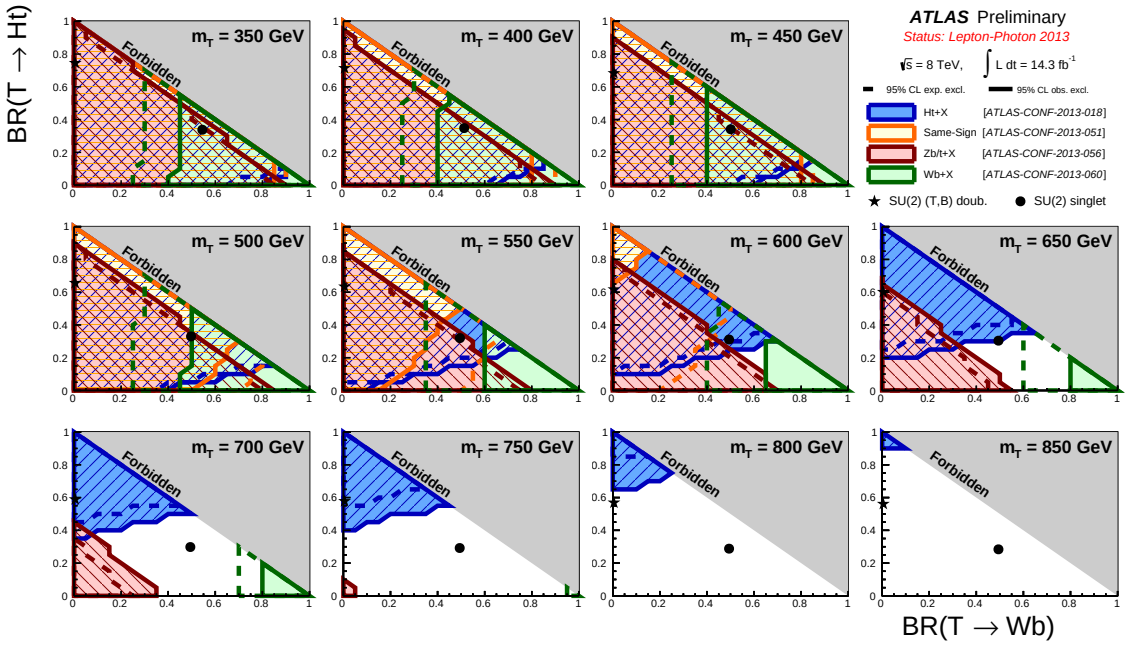

Figure 13: Summary plot showing the excluded branching ratios for different masses of vector like T quarks [5].

4. Heavy Ion Physics

There have been several data taking periods with heavy ions giving many results: Pb-Pb col-

lisions at the center of mass energy per nucleon of 2.76 TeV, corresponding to an integrated luminosity of 160 μb^{-1}, were recorded in 2010 and 2011. During a short pilot run in september 2012, proton-Pb collisions were recorded when a 4 TeV proton beam collided with a 1.57 TeV per nucleon Pb beam, resulting in 1 μb^{-1} of integrated luminosity. 30 nb^{-1} of p-Pb collisions at 5.02 TeV were recorded in the beginning of 2013. Some of the results included the measurement of centrality, charged hadron suppression, boson-jet correlation, jet fragmentation and the study of the azimuthal dependence of jet suppression, and scaling of Z production with collision centrality (number of binary collisions), in three p_T ranges.

With the proton-lead collisions, two particle correlation functions were studied, showing an enhanced production of pairs of particles at $\Delta\phi = 0$ (where $\Delta\phi = \phi_a - \phi_b$ for 2 particles a and b), with the correlations extending over a large range in $\Delta\eta$ (this is called "the ridge"). Such correlations have also been seen in p-p and Pb-Pb collisions. To provide further insight into the origin of this effect, these long range correlations have been studied in relative azimuthal angle $\Delta\phi$ and pseudorapidity $\Delta\eta$ in terms of the ratio $C(\Delta\phi,\Delta\eta) = \frac{S(\Delta\phi,\Delta\eta)}{B(\Delta\phi,\Delta\eta)}$, where $\Delta\phi$, $\Delta\eta = \eta_a - \eta_b$ represent pair distributions of 2 particles a and b constructed from same (S) and mixed (B) events [30]. For the first time, an "away side" correlation, located at $\Delta\phi = \pi$ has been observed and is shown in figure 14. Such correlations have been predicted in color glass condensate models.

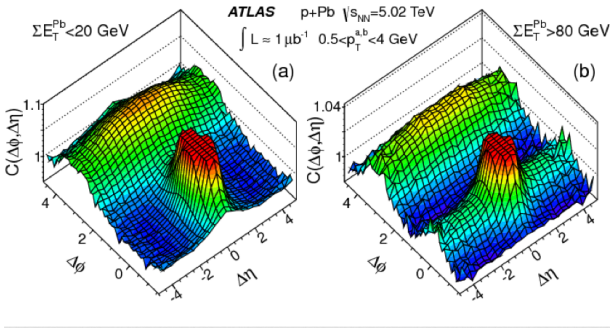

Figure 14: Two particle correlations in P-Pb collisions, for peripheral (a) and central (b) events, both truncated to suppress the large correlations at (0,0). The away side correlation is seen at $\Delta\phi = \pi$ [30].

5. Conclusion

The last four years have been very fruitful times for the ATLAS collaboration, with both excellent LHC machine and detector performance, high efficiencies of data taking, computing and physics analyses. New measurements are probing observables at an unprecedented level of accuracy and in never before exploited phase space regions. In many analysis, the systematic uncertainties are becoming the limiting factors and we can say that we are entering an era of precision measurements at the LHC. Searches for physics beyond the Standard Model have been performed in a large number of final states topologies and theoretical scenarios. Overall, all the results are consistent with the Standard Model, with no clear evidence for new physics. After a shutdown, the new run will start in 2015 for LHC and for ATLAS, when the center of mass energy of about 13 TeV will be reached. This new energy frontier will give many new results and hopefully new surprises.

I would like to thank the conference organizers for a very pleasant conference, with a very nice atmosphere.

References

[1] ATLAS Collaboration, JINST 3 (2008) S08003

[2] L. Evans and P. Bryant, JINST 3 (2008) S08001

[3] Ilya Tsukermann, these proceedings

[4] https://twiki.cern.ch/twiki/bin/view/AtlasPublic

[5] https://twiki.cern.ch/twiki/bin/view/AtlasPublic/CombinedSummaryPlots

[6] ATLAS Collaboration, arXiv:1304.4739

[7] ATLAS Collaboration, ATLAS-CONF-2013-041, http://cds.cern.ch/record/1543225

[8] ATLAS Collaboration, ATLAS-CONF-2013-022, http://cds.cern.ch/record/1525723

[9] ATLAS Collaboration, ATLAS-CONF-2013-023, http://cds.cern.ch/record/1525728

[10] ATLAS Collaboration, Eur. Phys. Jour. C73 2509 (2013).

[11] ATLAS Collaboration, ATLAS-CONF-2013-043, http://cds.cern.ch/record/1544035

[12] ATLAS Collaboration, ATLAS-CONF-2013-020, http://cds.cern.ch/record/1525555

[13] ATLAS Collaboration, ATLAS-CONF-2013-021, http://cds.cern.ch/record/1525557

[14] ATLAS Collaboration, JHEP 03 (2013)128.

[15] ATLAS Collaboration, ATLAS-CONF-2012-157, http://cds.cern.ch/record/1493586

[16] J. Campbell, K. Ellis, and C. Williams, JHEP 1107 (2011) 018

[17] ATLAS Collaboration, ATLAS-CONF-2012-149, http://cds.cern.ch/record/1493488

[18] ATLAS Collaboration, ATLAS-CONF-2012-132, http://cds.cern.ch/record/1478371,
ATLAS Collaboration, ATLAS-CONF-2012-056, http://cds.cern.ch/record/1453783

[19] ATLAS Collaboration, ATLAS-CONF-2013-046, http://cds.cern.ch/record/1547327

[20] ATLAS Collaboration, ATLAS-CONF-2013-033, http://cds.cern.ch/record/1527531

[21] ATLAS Collaboration, ATLAS-CONF-2012-057, http://cds.cern.ch/record/1453785

[22] S. Frixione and B.R. Webber, JHEP 0206 (2002)

[23] ATLAS Collaboration, ATLAS-CONF-2013-038, http://cds.cern.ch/record/1537961

[24] ATLAS Collaboration, ATLAS-CONF-2013-047, http://cds.cern.ch/record/1547563

[25] ATLAS Collaboration, ATLAS-CONF-2013-061, http://cds.cern.ch/record/1557778

[26] ATLAS Collaboration, ATLAS-CONF-2013-035, http://cds.cern.ch/record/1532426

[27] ATLAS Collaboration, ATLAS-CONF-2012-148, http://cds.cern.ch/record/1493487

[28] ATLAS Collaboration, ATLAS-CONF-2013-017, http://cds.cern.ch/record/1525524

[29] ATLAS Collaboration, ATLAS-CONF-2013-015, http://cds.cern.ch/record/1525522

[30] ATLAS Collaboration, Phys. Rev. Lett 110, 182302 (2013).